Science Advances
AAAS

advances.sciencemag.org/cgi/content/full/5/5/eaau7459/DC1

Supplementary Materials for

Evolutionary parallelisms of pectoral and pelvic network-anatomy from fins to limbs

Borja Esteve-Altava*, Stephanie E. Pierce, Julia L. Molnar, Peter Johnston, Rui Diogo, John R. Hutchinson

*Corresponding author. Email: borja.esteve@upf.edu

Published 8 May 2019, *Sci. Adv.* **5**, eaau7459 (2019)
DOI: 10.1126/sciadv.aau7459

This PDF file includes:

Table S1. Model fitting of SURFACE estimations (wAIC).
Table S2. Result of the robustness test.
Table S3. Summary of the community structure search in anatomical networks.
Table S4. First and last appearance dates used to calibrate the phylogeny.
Table S5. Internal nodes used to constrain the calibrated phylogeny.
Table S6. Values of network variables measured on each extended network model.
Fig. S1. Estimated evolutionary shifts using SURFACE.
Fig. S2. Topological DTT for pectoral and pelvic appendages.
Fig. S3. Visual representation of network parameters [from (*23*)].
Fig. S4. Diagnostic plots of pGLS model assumptions for the number of nodes.
Fig. S5. Diagnostic plots of pGLS model assumptions for the number of links.
Fig. S6. Diagnostic plots of pGLS model assumptions for the density.
Fig. S7. Diagnostic plots of pGLS model assumptions for the clustering coefficient.
Fig. S8. Diagnostic plots of pGLS model assumptions for the shortest path length.
Fig. S9. Diagnostic plots of pGLS model assumptions for the heterogeneity.
Fig. S10. Diagnostic plots of pGLS model assumptions for the assortativity.
Fig. S11. Diagnostic plots of pGLS model assumptions for the parcellation.
Fig. S12. Biplots of the first two PCA components of topological variables for pectoral (circles) and pelvic (triangles) appendages combined.
Fig. S13. Estimated evolutionary shifts using SURFACE.
Fig. S14. Topological DTT for pectoral and pelvic appendages.
Fig. S15. Testing the pectoral-pelvic similarity bottleneck hypothesis for Tetrapoda.
Supplementary Methods
Supplementary Results
References (*67–104*)

SUPPLEMENTARY TABLES

Table S1. Model fitting of SURFACE estimations (wAIC).

	Pectoral appendage		Pelvic appendage	
	Entire sample	**Subsample**	**Entire sample**	**Subsample**
BM 1-rate	6e-4	3.6e-6	1e-5	6.9e-6
BM multi-rate	0.31	0.9	0.36	0.01
OU 1-regime	0.5	6.9e-3	1e-15	6.5e-13
OU multi-sigma & theta	0.017	0.01	0.05	0.18
OU multi-theta	0.17	0.07	0.59	0.8

Table S2. Result of the robustness test.

Appendage	Taxa / Parameter	N	K	D	C	L	H	A	P
Pectoral	*Mus*	FALSE	FALSE	TRUE	TRUE	TRUE	TRUE	TRUE	TRUE
	Didelphis	FALSE	FALSE	TRUE	TRUE	TRUE	TRUE	TRUE	TRUE
	Iguana	FALSE	FALSE	TRUE	TRUE	TRUE	TRUE	TRUE	TRUE
	Sphenodon	FALSE	FALSE	TRUE	TRUE	TRUE	TRUE	TRUE	TRUE
	Hyloplesion	FALSE	FALSE	TRUE	TRUE	TRUE	TRUE	TRUE	TRUE
	Pantylus	FALSE	FALSE	TRUE	TRUE	TRUE	TRUE	TRUE	TRUE
	Seymouria	FALSE	FALSE	TRUE	TRUE	TRUE	TRUE	TRUE	TRUE
	Ambystoma	FALSE	FALSE	TRUE	TRUE	TRUE	TRUE	TRUE	TRUE
	Salamandra	FALSE	FALSE	TRUE	TRUE	TRUE	TRUE	TRUE	TRUE
	Celtedens	FALSE	FALSE	TRUE	TRUE	TRUE	TRUE	TRUE	TRUE
	Eryops	FALSE	FALSE	TRUE	TRUE	TRUE	TRUE	TRUE	TRUE
	Balanerpeton	FALSE	FALSE	TRUE	TRUE	TRUE	TRUE	TRUE	TRUE
	Tulerpeton	FALSE	FALSE	TRUE	TRUE	TRUE	TRUE	TRUE	TRUE
	Tiktaalik	FALSE	FALSE	TRUE	TRUE	TRUE	TRUE	TRUE	TRUE
	Panderichthys	FALSE	FALSE	TRUE	TRUE	TRUE	TRUE	TRUE	TRUE
	Mandageria	FALSE	FALSE	TRUE	TRUE	TRUE	TRUE	TRUE	TRUE
	Cabonnichthys	FALSE	FALSE	TRUE	TRUE	TRUE	TRUE	TRUE	TRUE
	Eusthenopteron	FALSE	FALSE	TRUE	TRUE	TRUE	TRUE	TRUE	TRUE
	Gogonasus	FALSE	FALSE	TRUE	TRUE	TRUE	TRUE	TRUE	TRUE
	Sterropterygion	FALSE	FALSE	TRUE	TRUE	TRUE	TRUE	TRUE	TRUE
	Sauripterus	FALSE	FALSE	TRUE	TRUE	TRUE	TRUE	TRUE	TRUE
	Neoceratodus	FALSE	FALSE	TRUE	TRUE	TRUE	TRUE	TRUE	TRUE
	Latimeria	FALSE	FALSE	TRUE	TRUE	TRUE	TRUE	TRUE	TRUE
	Polypterus	FALSE	FALSE	TRUE	TRUE	TRUE	TRUE	TRUE	TRUE
	Mus	FALSE	FALSE	TRUE	TRUE	TRUE	TRUE	TRUE	TRUE

	Didelphis	FALSE	FALSE	TRUE	TRUE	TRUE	TRUE	TRUE	FALSE
	Iguana	FALSE	FALSE	TRUE	TRUE	TRUE	TRUE	TRUE	TRUE
	Sphenodon	FALSE	FALSE	TRUE	TRUE	TRUE	TRUE	TRUE	TRUE
	Hyloplesion	FALSE	FALSE	TRUE	TRUE	TRUE	TRUE	TRUE	FALSE
	Pantylus	FALSE	FALSE	TRUE	TRUE	TRUE	TRUE	TRUE	TRUE
	Westlothiana	FALSE	FALSE	TRUE	TRUE	TRUE	TRUE	TRUE	FALSE
	Seymouria	FALSE	FALSE	TRUE	TRUE	TRUE	TRUE	TRUE	TRUE
	Ambystoma	FALSE	FALSE	TRUE	TRUE	TRUE	TRUE	TRUE	TRUE
	Salamandra	FALSE	FALSE	TRUE	TRUE	TRUE	TRUE	TRUE	TRUE
	Celtedens	FALSE	FALSE	TRUE	TRUE	TRUE	TRUE	TRUE	TRUE
	Eryops	FALSE	FALSE	TRUE	TRUE	TRUE	TRUE	TRUE	TRUE
	Balanerpeton	FALSE	FALSE	TRUE	TRUE	TRUE	TRUE	TRUE	TRUE
Pelvic	*Tulerpeton*	FALSE	FALSE	TRUE	TRUE	TRUE	TRUE	TRUE	TRUE
	Ichthyostega	FALSE	FALSE	TRUE	TRUE	TRUE	TRUE	TRUE	TRUE
	Acanthostega	FALSE	FALSE	TRUE	TRUE	TRUE	TRUE	TRUE	TRUE
	Panderichthys	FALSE	FALSE	TRUE	TRUE	TRUE	TRUE	TRUE	TRUE
	Eusthenopteron	FALSE	FALSE	TRUE	TRUE	TRUE	TRUE	TRUE	TRUE
	Sterropterygion	FALSE	FALSE	TRUE	TRUE	TRUE	TRUE	TRUE	TRUE
	Neoceratodus	FALSE	FALSE	TRUE	FALSE	FALSE	TRUE	TRUE	TRUE
	Latimeria	FALSE	FALSE	TRUE	TRUE	TRUE	TRUE	TRUE	TRUE
	Polypterus	FALSE	FALSE	TRUE	TRUE	TRUE	TRUE	TRUE	TRUE

* TRUE means that the observed value of this parameter in this anatomical network was not different from the average measured in the sample of 10,000 noisy networks with artificially generated errors.

SUPPLEMENTARY FIGURES

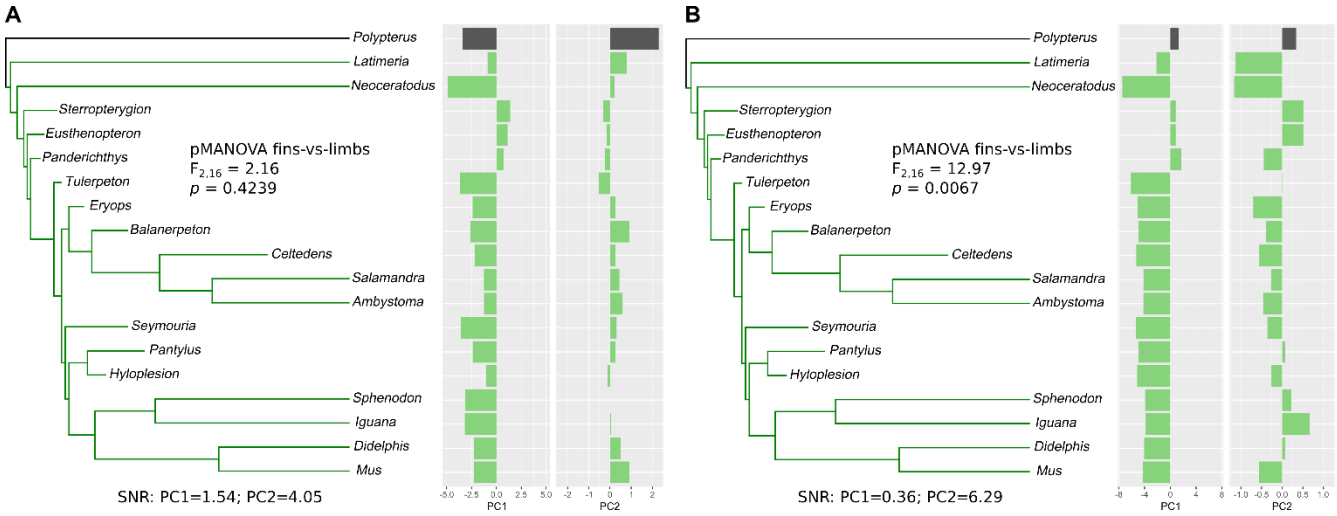

Fig. S1. Estimated evolutionary shifts using SURFACE. (**A**) Estimation using the subsample of pectoral appendages having both appendages represented in the sample. (**B**) Estimation using the subsample of pelvic appendages having both appendages represented in the sample. Details in Fig. 3.

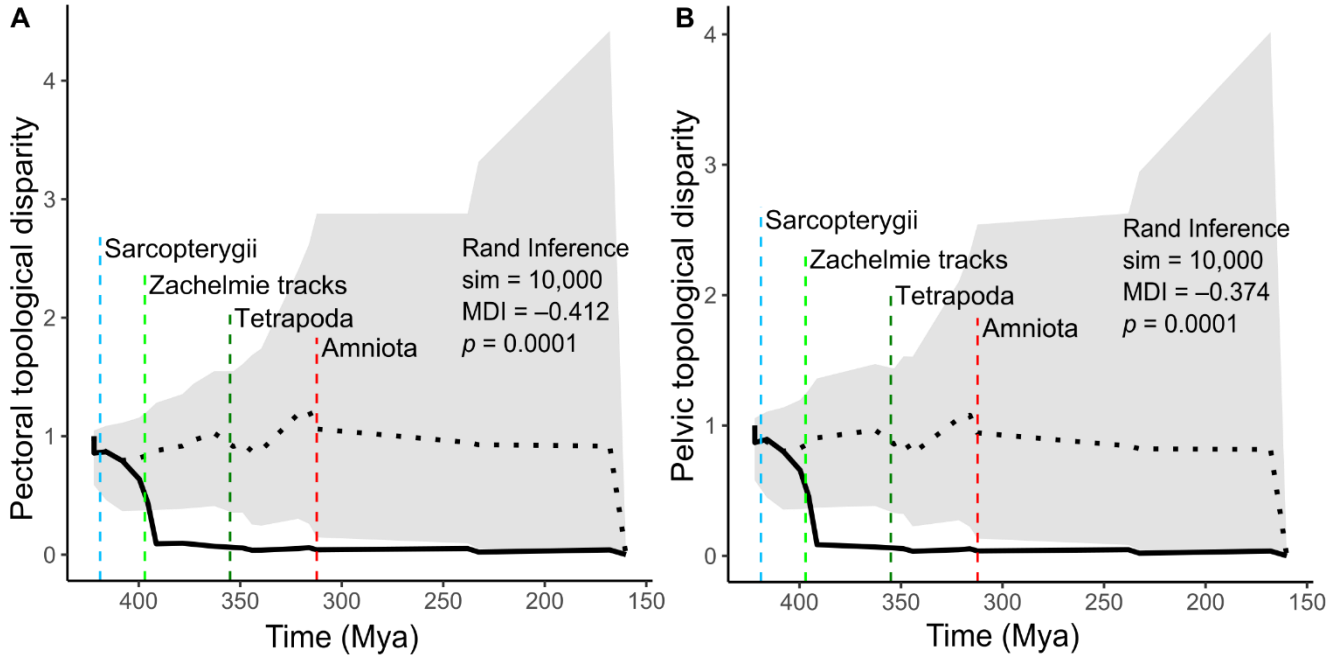

Fig. S2. Topological DTT for pectoral and pelvic appendages. (**A**) Pectoral subsample. (**B**) Pelvic subsample. Details in Fig. 5.

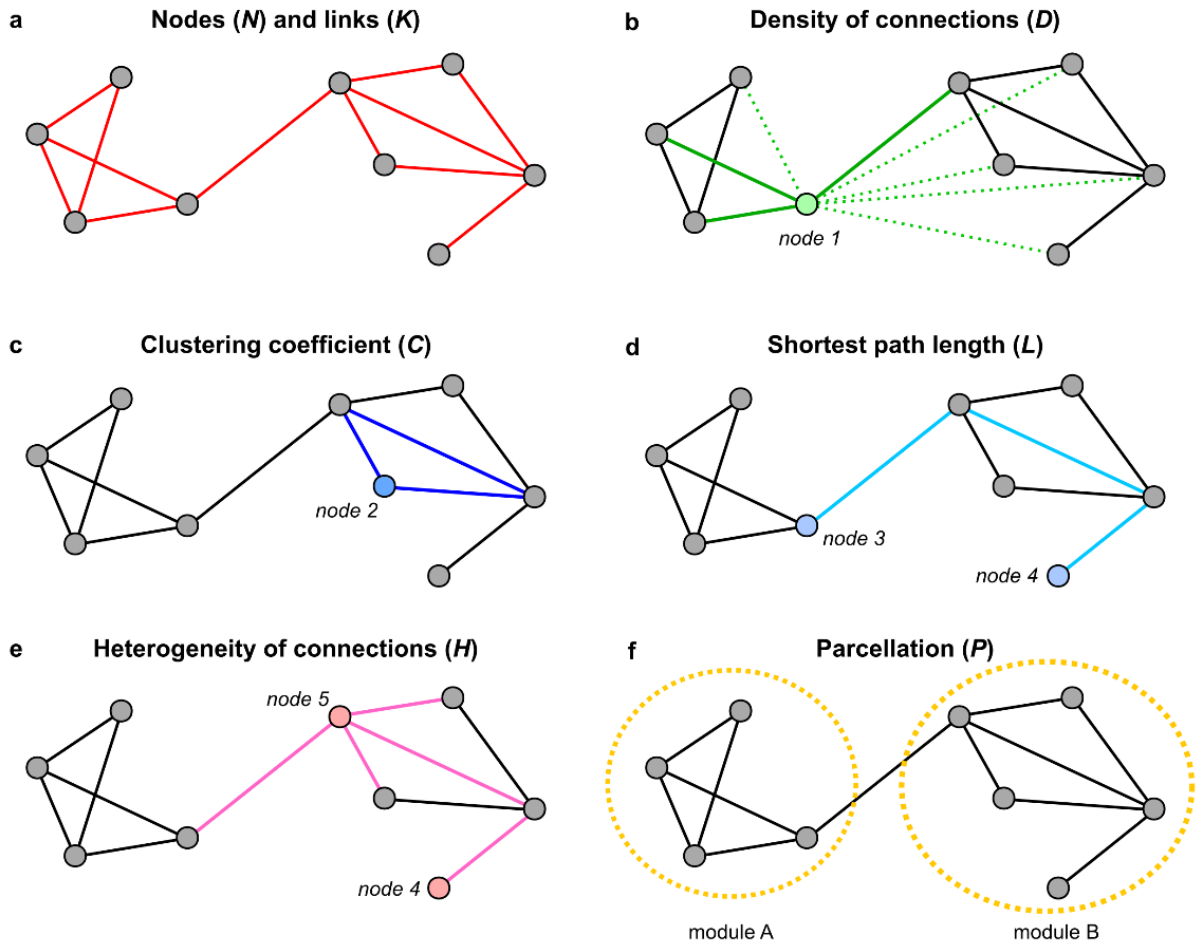

Fig. S3. Visual representation of network parameters [from (*23*)]. (A) Number of nodes (*grey dots*; N=9) and number of links (*red lines*; K=12). **(B)** Density (D) is calculated for the entire network; here we show an example with only one node: it has three connections (*solid green*) and five possible but not realized connections (*dashed green*); thus, D_{node1}=3/8. **(C)** Mean clustering coefficient (C) is calculated for the entire network; here we show an example with only one node. Node 2 (*in blue*) has only two neighbours, which are in turn connected to each other (*solid blue*), forming a 3-node loop or triangle. Because all neighbours of node 2 are connected among them, C_{node2}=1. **(D)** Mean path length (L) is calculated for the entire network; here we show an example with only two nodes. Three links (*in cyan*) are the minimum number of links required to connect node 3 and node 4; thus, $L_{node3,\ node4}$=3. **(E)** Heterogeneity of connections (H) is calculated for the entire network; here we show an example with only two nodes. Nodes 4 and 5 have a different number of connections, one and four, respectively. If we only consider these two nodes, then H≈2.1/2.5=0.84. **(F)** Parcellation (P) is calculated after a community detection algorithm has identified the connectivity modules; two in this example: module A and module B (dashed yellow circles). Module A has four nodes and module B has five nodes of a total of nine nodes in the network; thus, P=1–[(4/9)2+(5/9)2]=0.49. If the network were divided less uniformly, for example, into one large module of seven nodes and one small module of two nodes, then P=1–[(7/9)2+(2/9)2]=0.35. In contrast, if the nine nodes of the network were divided into three modules of equal size (i.e., three 3-node modules), then P=1–[(3/9)2+(3/9)2+(3/9)2]=0.67. Finally, assortativity of connections (A) is best visualized as a correlation coefficient of nodes connecting more frequently to nodes with the same number of connections (positive correlation) or to nodes with a different number of connections (negative correlation).

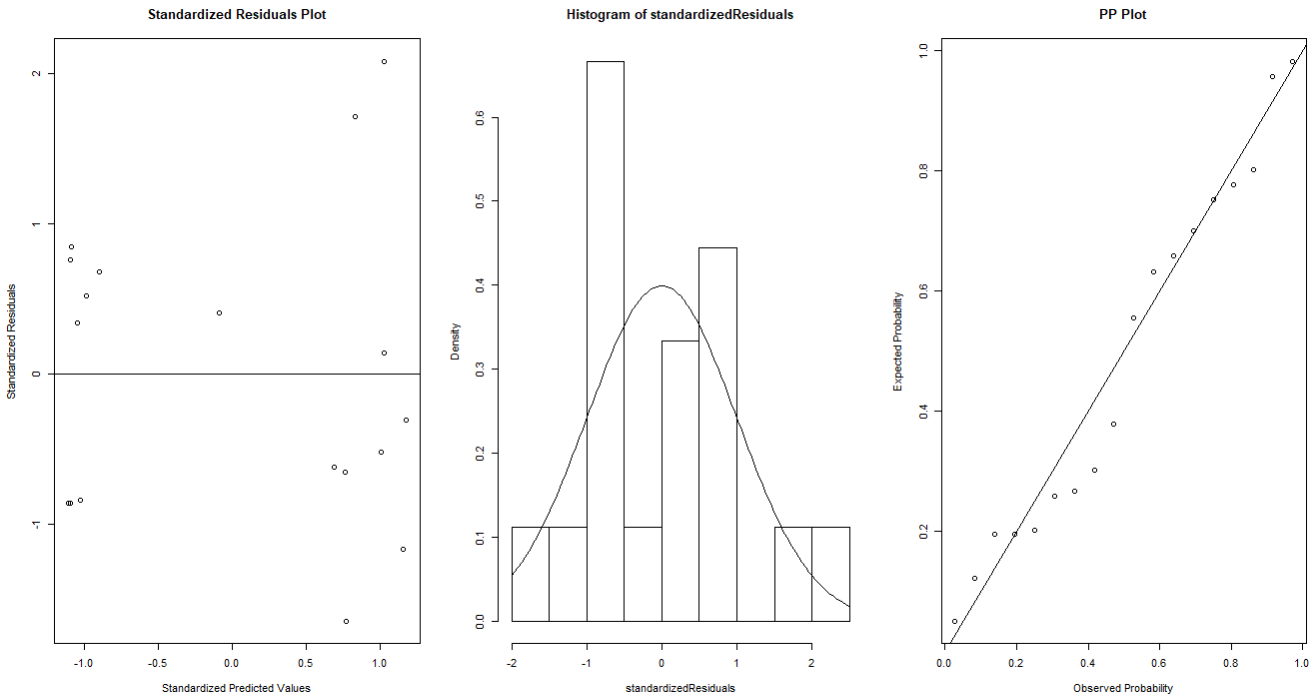

Fig. S4. Diagnostic plots of pGLS model assumptions for the number of nodes.

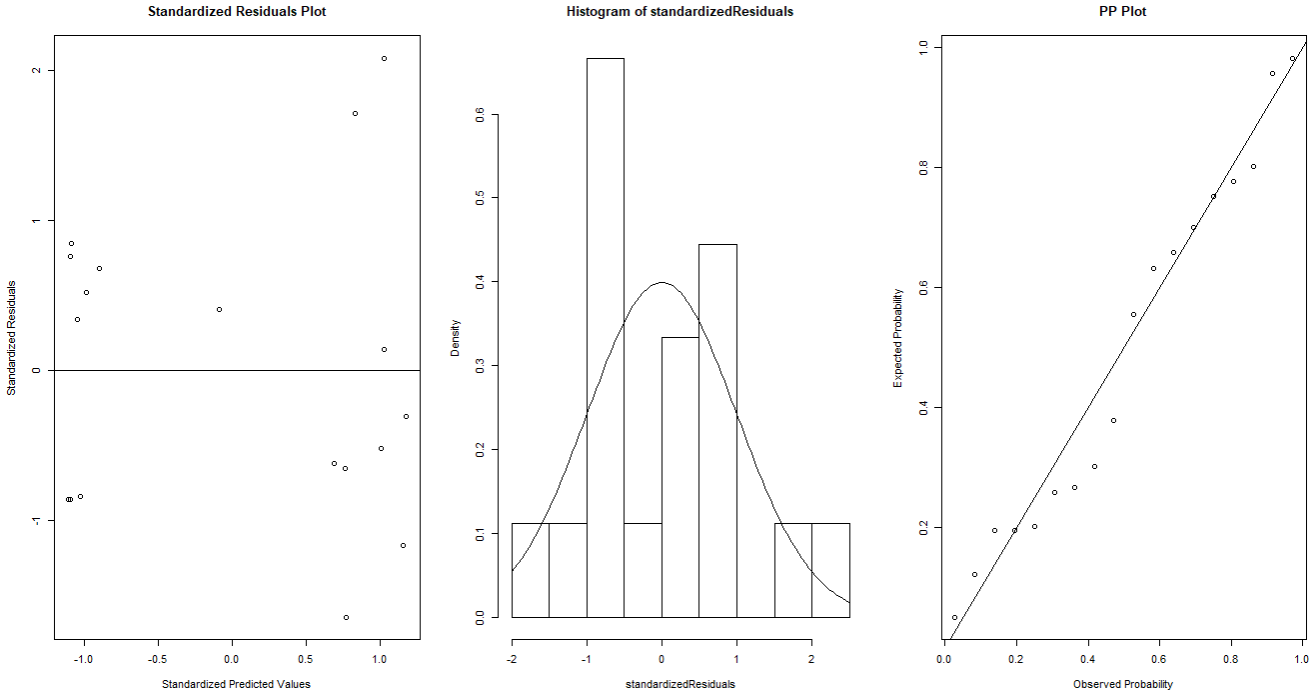

Fig. S5. Diagnostic plots of pGLS model assumptions for the number of links.

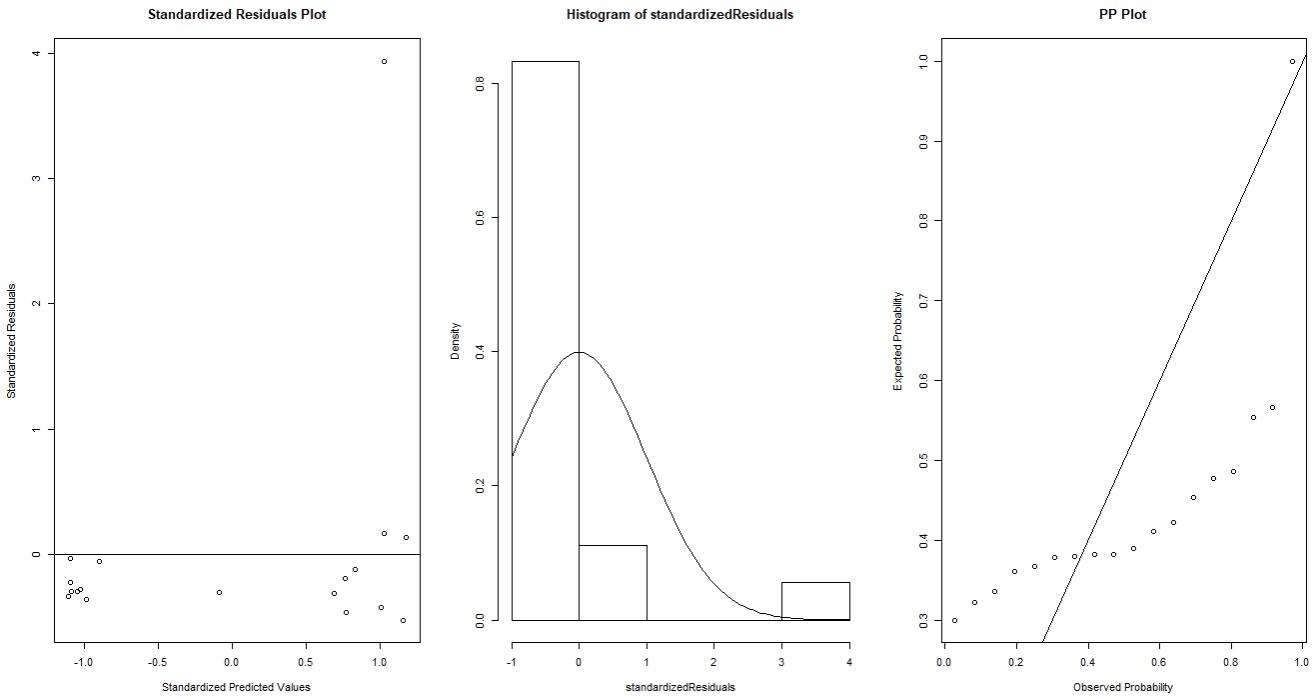

Fig. S6. Diagnostic plots of pGLS model assumptions for the density.

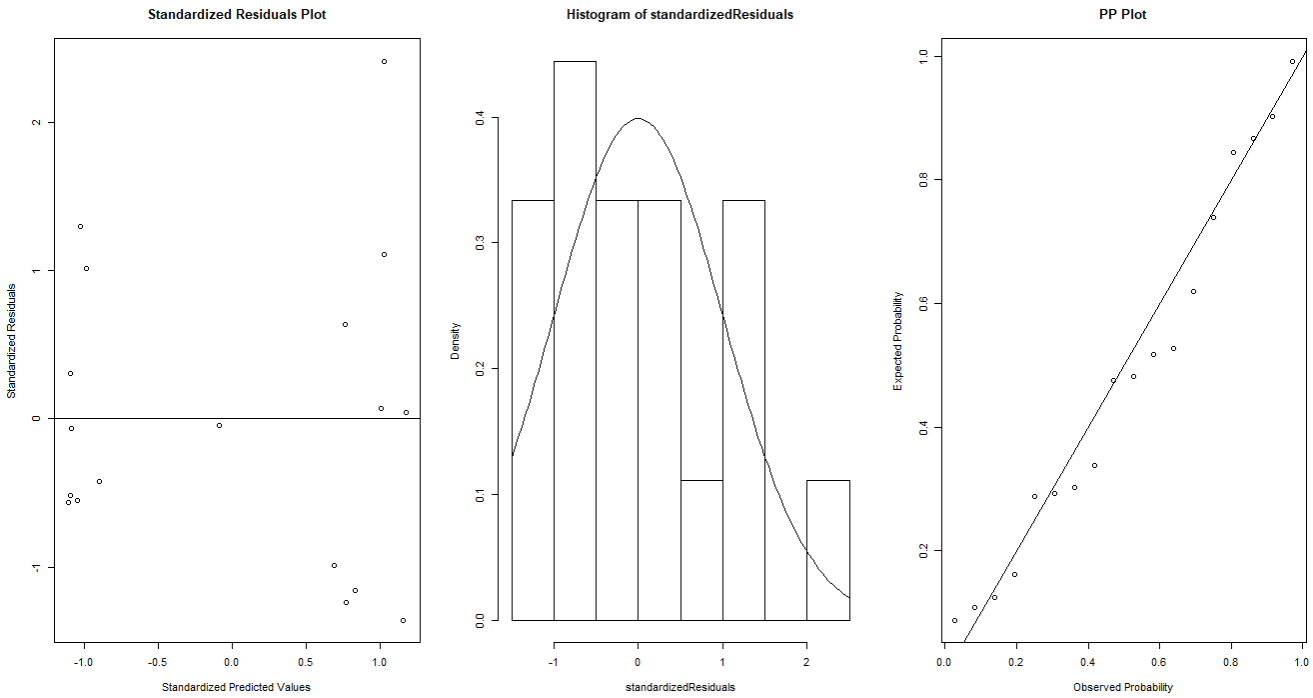

Fig. S7. Diagnostic plots of pGLS model assumptions for the clustering coefficient.

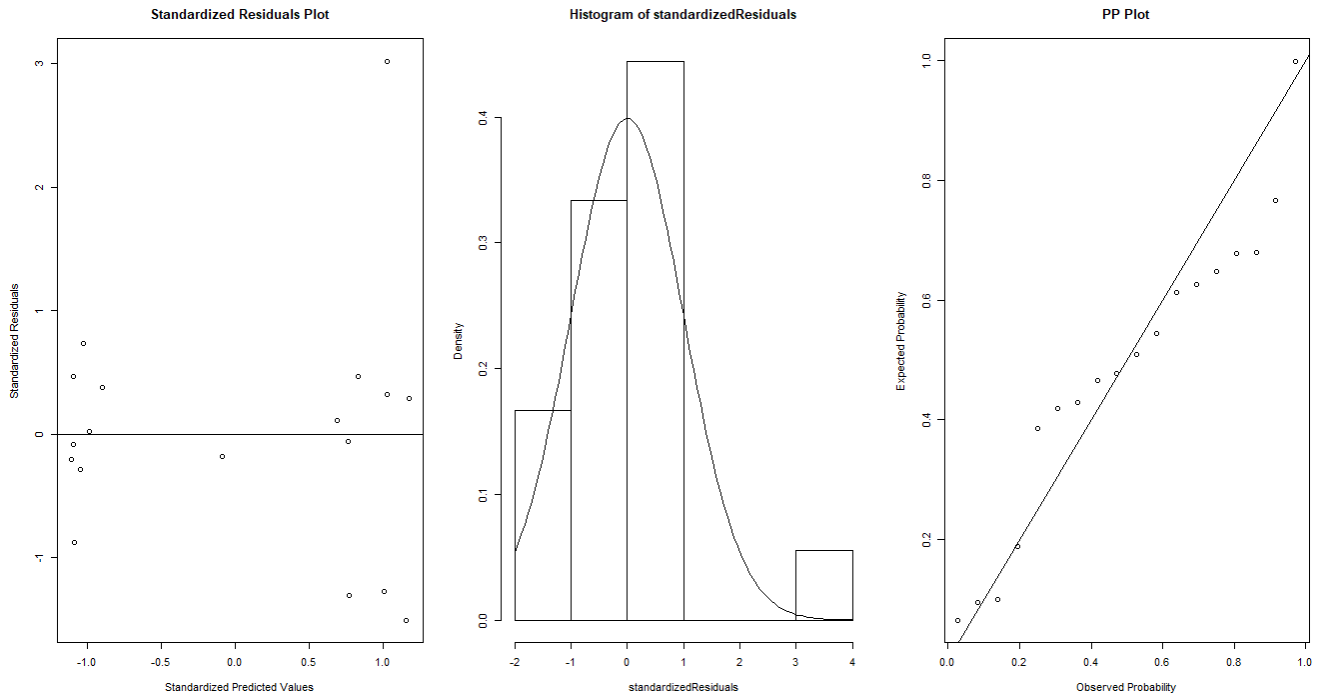

Fig. S8. Diagnostic plots of pGLS model assumptions for the shortest path length.

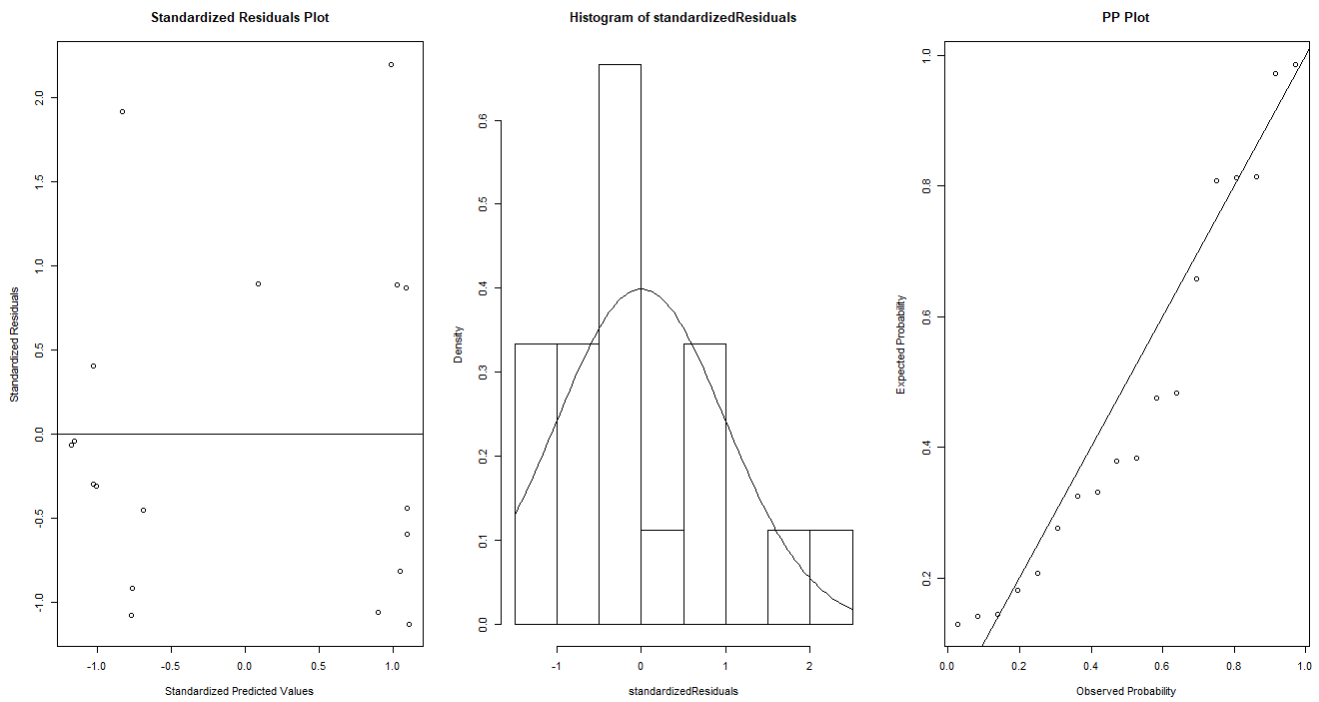

Fig. S9. Diagnostic plots of pGLS model assumptions for the heterogeneity.

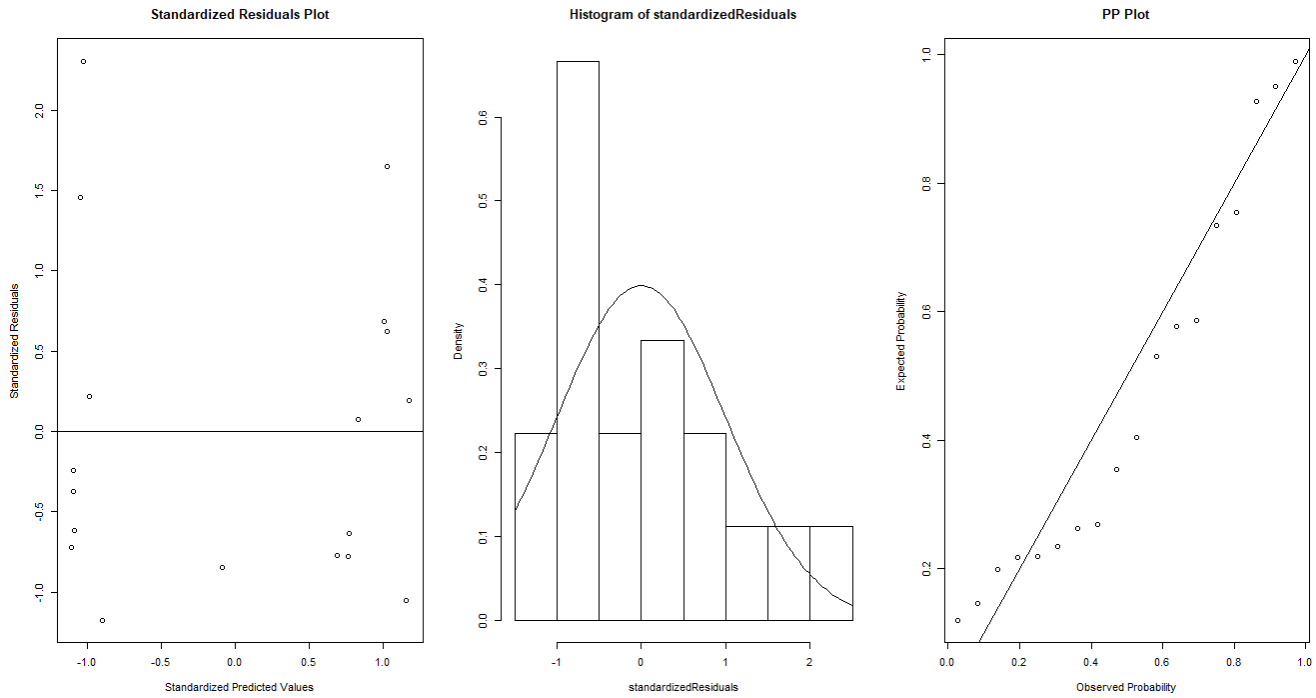

Fig. S10. Diagnostic plots of pGLS model assumptions for the assortativity.

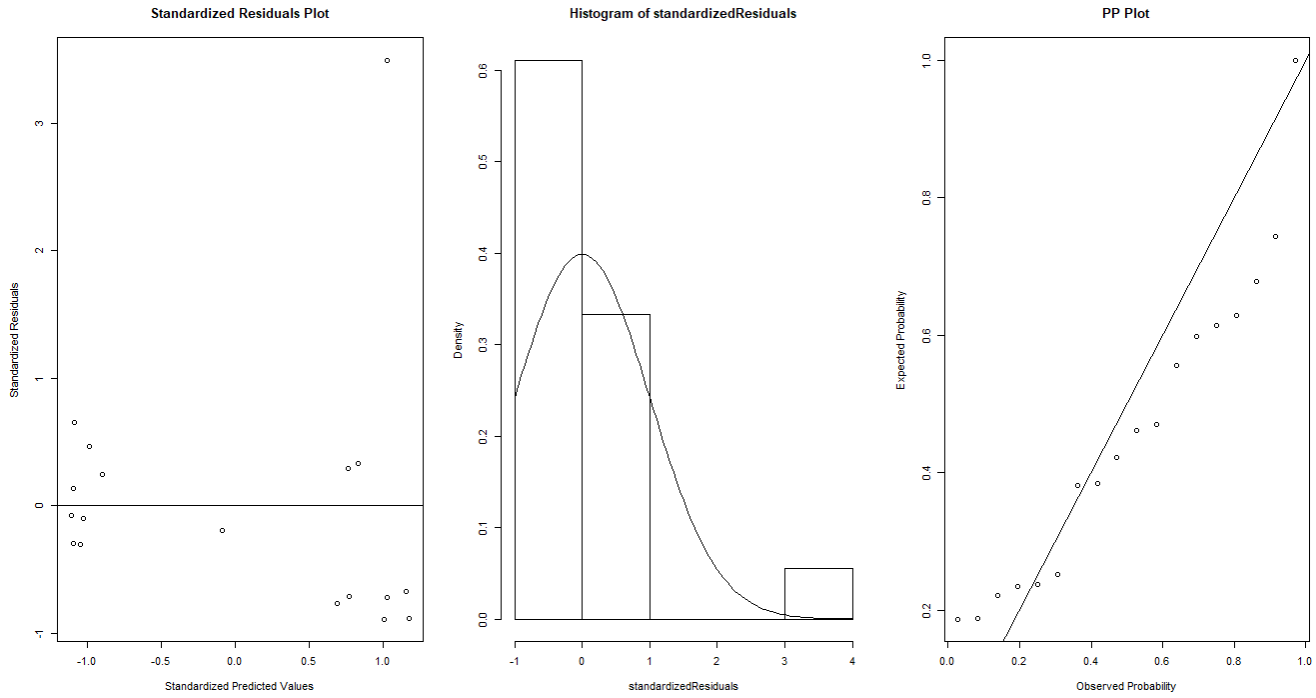

Fig. S11. Diagnostic plots of pGLS model assumptions for the parcellation.

SUPPLEMENTARY METHODS

Abbreviations of Museum Collections

AMF: Australian Museum, Sydney (Australia). AMNH: American Museum of Natural History, New York (USA). BMNH: British Museum of Natural History, London (UK). GIT: Institute of Geology, University of Technology, Tallinn (Latvia). GLAHM Hunterian Museum, Glasgow University, Glasgow (UK). LH: Las Hoyas, Madrid (Spain). MCZ Museum of Comparative Zoology, Harvard University, Cambridge (USA). MGUH: Museum Geologicum Universitatis Hafniensis, Copenhagen (DEN). NMS G Department of Geology, National Museums of Scotland, Edinburgh (UK). NMV: National Museum Victoria, Melbourne (AUS). MNG: Museum der Natur, Gotha (GER). NUFV: Nunavut Fossil Vertebrate Collection, Chicago (USA). PIN: Paleontological Institute, Russian Academy of Sciences, Moscow (RUS). RSM: Royal Scottish Museum, Edinburgh (UK). SMNH: Naturhistoriska Riksmuseet, Stockholm (SWE). UMZC (OS): University Museum of Zoology, Cambridge (UK). UT: University of Texas, Austin (USA). W: Westoll Collection at the Department of Geology, University of Newcastle (UK). WAM: Western Australian Museum, Perth (AUS).

Anatomical Information and Specimen Reference

The pectoral network of *Sauripterus* was coded following Davis et al.'s (*67*, *68*) description and reassessment of the holotype (AMNH 3341) based on specimens ANSP 20581, 20980 and 20981. To build the minimal network, we used their original reconstruction (*ibid.* Fig. 3), which includes only proximodistal contacts; for completeness we added the missing preaxial distal radial originating from the second radial. To build the extended network, we added the following mediolateral contacts between: (*i*) radius and ulna; (*ii*) radius and intermedium; (*iii*) intermedium and radial 2; (*iv*) radial 1 and radial 2; (*v*) preaxial distal radial 3 and postaxial distal radial 3; (*vi*) radial 7 and radial 8; and (*vii*) preaxial distal radial 8 and postaxial distal radial 8.

The pectoral network of *Sterropterygion* was coded following Thomson's (*69*) and Rackoff's (*70*) descriptions of the holotype and sole known specimen YPM VP.006721. To build the minimal network, we used the image provided by Thompson (*ibid.* Fig. 4). To build the extended network, we added mediolateral contacts between the ulnare and intermedium. Because the pectoral girdle is not well

preserved, we coded it as it is found in *Gogonasus*, which is its closest known relative. For this reason, results regarding the similarity of both taxa should be interpreted with some caution.

The pelvic network of *Sterropterygion* was coded following Thomson's (*69*) and Rackoff's (*70*) descriptions of the holotype and sole known specimen YPM VP.006721, and Thomson's acknowledgement that the internal fin skeleton only differs from that of *Eusthenopteron* in the relative proportions of elements (*ibid.* Fig. 5). Thus, minimal and extended networks were coded equal to those of *Eusthenopteron*. For this reason, results regarding the similarity of these taxa should be interpreted with caution.

The pectoral network of *Gogonasus* was coded following descriptions by Long et al. (*71*, *72*) and Holland (*73*) of specimens NMV P221807 and WAM 86.9.661. To build the minimal network, we used their original reconstruction (*ibid.* Long et al. Fig 2; *ibid.* Holland Figs. 2, 9), which includes a proximal mediolateral contact between the ulna and radius. For completeness, we added to the minimal network the interclavicle and the third distal radial, whose presence was presumed but not directly preserved. To build the extended network, we added the following mediolateral contacts between: (*i*) radius and intermedium; (*ii*) ulnare and intermedium; (*iii*) intermedium and distal radial 3; and (*iv*) axial mesomere 4 and distal radial 3.

The pectoral network of *Eusthenopteron* was coded following descriptions by Andrews and Westoll (*74*) based on a large number of specimens (e.g., BMNH P 60388, W 661, SMNH P.222, OS 2.5/7). To build the minimal network, we used their original reconstruction (*ibid.* Figs. 2-6), which includes the mediolateral contact between ulna and radius proximally, as it is found in large adult specimens; we also included the contact between cleithrum and clavicle as present. To build the extended network, we added the following mediolateral contacts between: (*i*) ulnare and preaxial radial 2; (*ii*) axial mesomere 4 and preaxial radial 3.

The pelvic network of *Eusthenopteron* was coded following descriptions by Andrews and Westoll (*74*) on several specimens (e.g., W 657, W 659, OS 2.5/20, RSM 1897.51.183). To build the minimal network, we used their original reconstruction (*ibid.* Fig. 17), which includes a not preserved, but

presumably present, cartilaginous prepubis, as suggested by the reconstruction's authors. No additional connections were included for the extended network.

The pectoral network of *Cabonnichthys* was coded following the description by Ahlberg and Johanson (*75*) of specimen AMF 9685a. To build the minimal network, we used their original reconstructions (*ibid.* Fig. 13). To build the extended network, we added the following mediolateral contacts between: (*i*) ulna and radius; and (*ii*) ulnare and intermedium.

The pectoral network of *Mandageria* was coded following the description by Johanson and Ahlberg (*76*) of specimens F96508, F96855, F96897a, and F96897b. To build the minimal network, we used their original reconstructions (*ibid.* Fig. 16) to which we added the interclavicle in the same configuration as in *Eusthenopteron*, which the girdle resembles greatly according to Johanson and Alhberg. To build the extended network, we added the following mediolateral contacts between: (*i*) ulnare and intermedium; (*ii*) axial mesomere 4 and preaxial radial 3.

The pectoral network of *Panderichthys* was coded following Boisvert et al.'s (*11*) descriptions based on specimen GIT434-1 (*ibid.* Figs. 2, 3) for the fin and Vorobyeva's (*77*) description of the girdle based on specimen PIN N3547/19 (*ibid.* Fig. 1). To build the minimal network, we included an interclavicle element and its connection to the chleithrum following Vorobyeva's inference although an interclavicle is not preserved. No additional connections were included for the extended network.

The pelvic network of *Panderichthys* was coded following Boisvert's (*12*) description of the fin based on specimen GIT434-1 (*ibid.* Figs. 1, 2). To build the minimal network we used the original description. No additional connections were included for the extended network.

The pectoral network of *Tiktaalik* was coded following Shubin et al.'s (*13, 78*,) descriptions based on specimens NUFV 108, 109, 110 and 112. To build the minimal network, we used their original reconstruction (*ibid.* Figs. 2, 3), which only includes proximodistal articulations between fin bones. To build the extended network, we added the following mediolateral contacts between: (*i*) radius and ulna;

(*ii*) radius and intermedium; (*iii*) intermedium and ulnare; (*iv*) proximal radial 2 and axial mesomere 4; (*v*) axial mesomere 4 and proximal radial 3; (*vi*) proximal radial 3 and proximal radial 4; (*vii*) intermedial radial 1 and axial mesomere 5; (*viii*) axial mesomere 5 and intermedial radial 1; and (*ix*) distal radial 1 and distal radial 2.

The pelvic network of *Acanthostega* was coded following Coates's (*79*) description based on specimens MGUH T1291, f.n. 1227 and f.n. 1375. To build the minimal network, we used his original reconstruction (*ibid.* Fig. 24). Note that a few elements of the carpus might be missing in the reconstruction due to lack of preservation. No additional connections were included for the extended network.

The pelvic network of *Ichthyostega* was coded following the descriptions by Coates and Clack (*80*) and Jarvik (*81*), based on specimen MGUH 1349. For the minimal network, we used the original reconstruction by Coates and Clack (*ibid.* Fig. 1), excluding the element of the pes described as a poorly ossified mass. To build the extended network, we added the following mediolateral contacts between: (*i*) distal tarsals 4 and 5; (*ii*) distal tarsals 5 and 6; and (*iii*) distal tarsals 6 and 7.

The pectoral network of *Tulerpeton* was coded following Lebedev and Coates's (*82*) description based on specimen PIN 2921. There was ambiguity in that description regarding the identity of "metacarpals" as either true metacarpals or metacarpal-like distal carpals. To build the minimal network, we used their original reconstruction (*ibid.* Figs. 3, 8), assuming that the bones were metacarpals (note that the alternative interpretation does not change the topology of the network model, as the contacts would be the same). To build the extended network, we added the following mediolateral contacts between: (*i*) metacarpals 1 and 2; (*ii*) metacarpals 2 and 3; (*iii*) metacarpals 3 and 4; and (*iv*) metacarpals 4 and 5.

The pelvic network of *Tulerpeton* was coded following Lebedev and Coates's (*82*) description based on specimen PIN 2921. To build the minimal network, we used their original reconstruction (*ibid.* Fig. 12), which includes inferred reconstruction of missing phalanges. For completeness, we also added the missing second tarsal bone, whose position can be inferred indirectly. As noted by Lebedev and Coates, the restoration of phalanges was made to resemble the phalangeal formula of the forelimb, which might

artificially increase the degree of similarity between pectoral and pelvic appendages for *Tulerpeton*. No additional connections were included for the extended network.

The pectoral network of *Balanerpeton* was coded following Miler & Sequeira's (*83*) description based on specimens GLAHM V2051, NMSG 1985.4.1, 1987.7.32 and UMZC T1313. To build the minimal network, we used their original reconstruction (*ibid.* Fig. 12), which includes the inferred ulnare, third central, and fourth distal carpal, since no specimen exhibits a complete articulated carpus. To build the extended network, we added the following mediolateral contacts between: (*i*) radius and ulna; (*ii*) radius and intermedium; and (*iii*) radiale and centrale 2.

The pelvic network of *Balanerpeton* was coded following Miler & Sequeira's (*83*) description based on specimens GLAHM V2052, NMSG 1985.4.1, 1985.232.1 and UMZC T1261, T1313. To build the minimal network, we used their original reconstruction (*ibid.* Fig. 15), which includes an inferred first central bone. No additional connections were included for the extended network.

The pectoral network of *Eryops* was coded following descriptions by Milner (*84*), Pawley and Warren(*85*), and Dilkes(*86*), based on many specimens (see *op. cit.*). To build the minimal network, we used the reconstructions of specimen AMNH 4186 girdle by Milner (*ibid.* Fig. 3) and carpus by Dilkes (*ibid.* Fig. 2A). No additional connections were included for the extended network.

The pelvic network of *Eryops* was coded following descriptions by Pawley and Warren (*85*) and Dilkes (*86*), based on many specimens (see *op. cit.*). To build the minimal network, we used the reconstructions of the girdle, stylopod and zeugopod by Pawley and Warren (*ibid*. Figs. 8-10) and of the autopod of specimen AMNH 4186 by Dilkes (*ibid.* Fig. 6D). To build the extended network, we added a mediolateral contact between centrale 2 and distal tarsal 3.

The pectoral network of *Celtedens* was coded following the description by McGowan (*87*), based on specimens LH6020 and LH030. To build the minimal network, we used the reconstructions by

McGowan (*ibid.* Fig. 8). To build the extended network, we added the following mediolateral contacts between: (*i*) radiale and intermedium; (*ii*) centrale 3 and carpal 2; and (*iii*) centrale 3 and carpal 3.

The pelvic network of *Celtedens* was coded following the description by McGowan (*87*), based on specimen LH6020. To build the minimal network, we used the reconstructions by McGowan (*ibid.* Fig. 11). No additional connections were included for the extended network.

The pectoral network of *Seymouria* was coded following descriptions by Romer (*88*), White (*89*), and Berman et al. (*90*), based on specimens MCZ 1094, 1643, 1650, and MNG 10553, 10554. To build the minimal network, we used the original reconstruction of the pelvic girdle of *S. baylorensis* by Romer (*ibid.* Fig. 143) and of the manus of *S. sanjuanensis* by Berman et al. (*ibid.* Fig. 7A). To build the extended network, we added the following mediolateral contacts between: (*i*) radius and intermedium; and (*ii*) centrale 1 and distal carpal 3.

The pelvic network of *Seymouria* was coded following descriptions by White (*89*) and Berman et al. (*90*), based on specimens MCZ 1099, 1644, 1661, and MNG 10553, 10554. To build the minimal network, we used the original reconstruction of the pelvic girdle of *S. baylorensis* by White (*ibid.* Figs 25, 26) and of the pedes of *S. sanjuanensis* by Berman et al. (*ibid.* Fig. 7B). To build the extended network, we added the mediolateral contacts between centrale 2 and distal tarsal 2.

The pelvic network of *Westlothiana* was coded following Smithson et al.'s (*91*) description based on specimens NMSG 1990.72.1 and 1991.47.1. To build the minimal network, we used their original reconstruction (*ibid.* Fig. 20), completed by Sumida's (*92*) interpretation (Fig. 16). To build the extended network, we added the following mediolateral contacts between: (*i*) tibia and fibula; (*ii*) tibiale and centrale 2; and (*iii*) fibulare and centrale 2.

The pectoral network of *Pantylus cordatus* was coded following Carroll and Gakill's (*93*) description based on specimens MCZ 3202 and UT 40001-6. To build the minimal network, we used their

reconstruction (*ibid*. Figs. 27, 29). To build the extended network, we added a mediolateral contact between metacarpals 3 and 4 as there seems to be some surface overlap between them.

The pelvic network of *Pantylus cordatus* was coded following Carroll and Gakill's (*93*) description based on specimen UT 40001-1. To build the minimal network, we used their reconstruction (*ibid*. Fig. 29). To build the extended network, we added a mediolateral contact between the tibia and the lateral os centrale, which is suspected but not certain.

The pectoral network of *Hyloplesion longicostatum* was coded following Carroll and Gakill's (*93*) description based on specimen RSM 1899.32.3. To build the minimal network, we used their reconstruction (*ibid*. Fig. 90). To build the extended network, we added mediolateral contacts (*i*) between the metacarpals, ulna and radius; and (ii) between metacarpal 2 and 3.

The pelvic network of *Hyloplesion longicostatum* was coded following Carroll and Gakill's (*93*) description based on specimen RSM 1899.32.3. To build the minimal network, we used their reconstruction (*ibid*. Fig. 90), which includes a not preserved, but inferred fifth tarsal bone. To build the extended network, we added a mediolateral contact between the tibia and the lateral os centrale, which is suspected but not certain. No additional connections were included for the extended network.

Details on our dissection of pectoral and pelvic appendages of the extant taxa *Polypterus*, *Latimeria*, *Neoceratodus*, *Ambystoma*, *Salamandra*, and *Sphenodon* were taken from Esteve-Altava *et al.*(*23*). For the present study we also included anatomical information on *Mus* from Rui Diogo's team's dissections (Howard University College of Medicine), *Didelphis* from dissections carried out by Diogo et al. (*94*), and *Iguana* from the literature (*95*).

Mathematical Description of Network Parameters

Anatomical networks were coded as adjacency matrices: square binary of dimension $N \times N$, where N represent the number of bones in the appendage, such that its element $M_{i.j}$ is 1 when there is a physical contact between bone i and bone j, and 0 when there is no physical contact.

The number of nodes (N) and of links ($K = \sum_{i=1}^{N} \sum_{j=i+1}^{N} M_{i,j}$) are count variables for the total number of bones and their physical contacts, respectively, as modeled in the anatomical network.

The density of connections (D) measures the ratio between the actual number of connections and the maximum number of connections possible, as $D = 2K/N(N-1)$. The value of D ranges from 0 to 1.

The mean clustering coefficient (C) measures the average of the ratio of a node's neighbors that connect among them, as $C = \frac{1}{N} \sum_{i=1}^{N} 2\tau_i / k_i(k_i - 1)$, where τ_i is the number of links connecting the nearest neighbors of node i and k_i are the nearest neighbors of (nodes connecting to) i. The value of C ranges from 0 to 1.

The mean path length (L) measures the average minimum number of links required to travel between two nodes, as $L = \frac{1}{N(N-1)} \sum_{i \neq j} l_{i,j}$, where $l_{i,j}$ is the shortest distance in links between nodes i and j (note that $l_{i,j} = 1$ when nodes i and j are connected). The minimal value of L is 1.

The heterogeneity of connections (H) measures the overall disparity of nodes for their number of connections, as $H = \sigma_k / \mu_k$, where σ_k is the standard deviation of the number of connections of all nodes in the network and μ_k is the mean of the number of connections per node. The minimal value of H is 0.

The assortativity of connections (A) measures the extent to which nodes with the same number of connections connect to each other, as $A = \frac{K^{-1}\sum_k i_k j_k - \left[K^{-1}\sum_k \frac{1}{2}(i_k + j_k)\right]^2}{K^{-1}\sum_k \frac{1}{2}(i_k^2 + j_k^2) - \left[K^{-1}\sum_k \frac{1}{2}(i_k + j_k)\right]^2}$, where i_k and j_k are the number of connections of nodes at the end of the link k. A behaves likewise the Pearson's correlation coefficient of the connections of nodes at either ends of a link; the value of A ranges between –1 and 1. Thus, A takes positive values when nodes with the same number of connections connect to each other, and it takes negative values otherwise.

The parcellation of the network (P) measures the extent to which the nodes of the network are divided into many balanced modules, as $P = 1 - \sum_{m=1}\left(\frac{N_m}{N}\right)^2$, where N_m is the number of nodes in module m. The value of P ranges from 0, when all nodes are in a same module, to 1 when nodes are evenly distributed within many modules.

Calculating P requires a previous identification of the partition of the network into modules. In this context, a module is a group of nodes with more links to nodes within the group than to nodes outside the group. We identified the best partition of the network using an optimization algorithm implemented in the function *cluster_optimal* of the R package *igraph*. This algorithm maximizes over all possible partitions the modularity measure defined by Newman and Girvan(*96*), as $Q = \sum_{s=1}^{m}\left[\frac{k_s}{K} - \left(\frac{d_s}{2K}\right)^2\right]$, where m is the number of modules of the partition, k_s is the number of links within module s, and d_s is the total number of links of nodes in s (both inside and outside s). In **table S3** we provide also the expected error of Q, which is calculated using a jackknife approach where each connection as an independent observation (*96*).

Table S3. Summary of the community structure search in anatomical networks.

Appendage	Taxon	# modules	Q $_{value}$	Q $_{expected\ error}$
Pectoral	Mus PECA	6	0.52	0.071
	Didelphis PECA	7	0.54	0.076
	Iguana PECA	8	0.61	0.068
	Sphenodon PECA	7	0.60	0.067

	Hyloplesion PECA	5	0.58	0.082
	Pantylus PECA	7	0.56	0.077
	Seymouria PECA	7	0.63	0.060
	Ambystoma PECA	5	0.49	0.082
	Salamandra PECA	6	0.49	0.089
	Celtedens PECA	7	0.60	0.068
	Eryops PECA	5	0.52	0.067
	Balanerpeton PECA	7	0.54	0.079
	Tulerpeton PECA	8	0.68	0.065
	Tiktaalik PECA	4	0.60	0.083
	Panderichthys PECA	4	0.53	0.098
	Mandageria PECA	4	0.49	0.125
	Cabonnichthys PECA	4	0.50	0.122
	Eusthenopteron PECA	3	0.51	0.100
	Gogonasus PECA	3	0.51	0.105
	Sterropterygion PECA	3	0.48	0.115
	Sauripterus PECA	5	0.67	0.061
	Neoceratodus PECA	7	0.68	0.048
	Latimeria PECA	5	0.58	0.073
	Polypterus PECA	7	0.52	0.063
Pelvic	Mus PELA	7	0.54	0.073
	Didelphis PELA	8	0.60	0.081
	Iguana PELA	5	0.65	0.070
	Sphenodon PELA	7	0.61	0.081
	Hyloplesion PELA	8	0.61	0.067
	Pantylus PELA	7	0.66	0.062
	Westlothiana PELA	7	0.62	0.069
	Seymouria PELA	7	0.61	0.061
	Ambystoma PELA	6	0.54	0.072
	Salamandra PELA	6	0.56	0.073
	Celtedens PELA	8	0.60	0.064
	Eryops PELA	7	0.58	0.069
	Balanerpeton PELA	7	0.58	0.066
	Tulerpeton PELA	7	0.64	0.055
	Ichthyostega PELA	8	0.66	0.060
	Acanthostega PELA	7	0.68	0.058
	Panderichthys PELA	2	0.13	0.179
	Eusthenopteron PELA	3	0.40	0.166
	Sterropterygion PELA	3	0.40	0.166
	Neoceratodus PELA	5	0.66	0.039
	Latimeria PELA	5	0.49	0.082
	Polypterus PELA	3	0.30	0.232

Phylogeny Topology & Calibration

For our comparative analyses we built a phylogenetic tree for our sample of taxa, which follows the most recent supertree assembled by Marcello Ruta and co-workers for early tetrapods (*54*), with the only exception of placing *Balanerpeton* as more basal than *Eryops*, for which there is consensus (*97–99*).

Table S4. First and last appearance dates used to calibrate the phylogeny.

Taxa	FAD (Ma)	LAD (Ma)
Polypterus	73	0
Latimeria	22	0
Neoceratodus	28.4	0
Sauripterus	361	358.9
Sterropterygion	361	358.9
Gogonasus	383.9	380
Eusthenopteron	387.2	375
Cabonnichthys	376.9	358.9
Mandageria	376.9	358.9
Panderichthys	387.2	380
Tiktaalik	383.9	376.1
Acanthostega	367.5	360.7
Ichthyostega	367.5	360.7
Tulerpeton	358	354
Balanerpeton	335	326.4
Eryops	297.2	272.5
Celtedens	167	100.5
Salamandra	12	0
Ambystoma	42	0
Seymouria	298.5	272.5
Westlothiana	335	326.4
Pantylus	285.9	251.9
Hyloplesion	308	298.9
Sphenodon	19	0
Iguana	13	0
Didelphis	12	0
Mus	10	0

Table S5. Internal nodes used to constrain the calibrated phylogeny.

Split *(phylogeny internal node)*	**Date (Ma)**	**Reference**
Actinopterygia—Sarcopterygia	419	(*100*) Zhu et al. 2009
Actinistia—Rhipidistia	416	(*101*) Swartz 2012
Dipnomorpha—Tetrapodomorpha	408	(*102*) Benton et al. 2015
Batrachomorpha—Reptiliomorpha	330.4	(*99*) Hedges & Kumar 2009, pg. 62
Synapsida—Diapsida	312.3	(*99*) Hedges & Kumar 2009, pg. 58
Rhynchocephalia—Squamata	238	(*103*) Jones et al. 2013
Treptobranchia—Salamandroidea	168	(*99*) Hedges & Kumar 2009, pg. 366
Marsupialia—Placentalia	160	(*104*) Luo et al. 2011

SUPPLEMENTARY RESULTS

We carried out the same anatomical network analysis and statistical comparisons described in the main text and Supplementary Methods for the extended version of appendages topology (see above). Here we summarized the main results by reproducing versions of the main tables and figures for the extended network models.

Table S6. Values of network variables measured on each extended network model.

Appendage	**Taxa**	**N**	**K**	**D**	**C**	**L**	**H**	**A**	**P**
	Mus	33	45	0.09	0.14	4.05	0.59	0.23	0.82
	Didelphis	32	42	0.08	0.16	4.38	0.55	0.46	0.84
	Iguana	38	47	0.07	0.12	5.21	0.49	0.55	0.86
	Sphenodon	37	47	0.07	0.13	5.24	0.50	0.61	0.84
	Hyloplesion	24	31	0.11	0.19	4.21	0.36	0.40	0.82
	Pantylus	32	43	0.09	0.18	4.53	0.48	0.50	0.85
	Seymouria	40	56	0.07	0.21	5.22	0.51	0.61	0.85
	Ambystoma	25	35	0.12	0.18	3.87	0.52	0.54	0.78
	Salamandra	25	34	0.11	0.16	4.00	0.53	0.55	0.82
	Celtedens	31	43	0.09	0.16	4.37	0.48	0.54	0.84
	Eryops	32	50	0.10	0.27	4.33	0.53	0.50	0.78
	Balanerpeton	32	45	0.09	0.15	4.63	0.51	0.66	0.82
Pectoral	*Tulerpeton*	42	51	0.06	0.07	5.45	0.45	0.61	0.86
	Tiktaalik	21	29	0.14	0.38	3.81	0.54	-0.10	0.75
	Panderichthys	15	17	0.16	0.27	3.64	0.42	-0.01	0.73
	Mandageria	13	16	0.21	0.46	3.12	0.39	-0.13	0.64
	Cabonnichthys	13	16	0.21	0.46	3.12	0.39	-0.13	0.64
	Eusthenopteron	14	17	0.19	0.38	3.31	0.42	-0.11	0.65
	Gogonasus	14	18	0.20	0.25	3.47	0.42	0.47	0.65
	Sterropterygion	13	14	0.18	0.22	3.33	0.50	-0.25	0.66
	Sauripterus	31	39	0.08	0.36	4.14	0.54	-0.03	0.78
	Neoceratodus	54	65	0.05	0.26	5.95	0.82	-0.59	0.85
	Latimeria	23	34	0.13	0.42	3.61	0.46	-0.12	0.78
	Polypterus	46	65	0.06	0.07	3.33	0.91	-0.13	0.85

	Mus	34	46	0.08	0.15	4.42	0.59	0.27	0.83
	Didelphis	33	38	0.07	0.10	4.80	0.53	0.39	0.87
	Iguana	30	32	0.07	0.08	5.27	0.40	0.50	0.80
	Sphenodon	31	36	0.08	0.12	4.91	0.51	0.40	0.85
	Hyloplesion	38	51	0.07	0.19	5.21	0.50	0.47	0.87
	Pantylus	37	47	0.07	0.16	5.24	0.46	0.47	0.85
	Westlothiana	37	48	0.07	0.13	5.33	0.51	0.66	0.85
	Seymouria	39	54	0.07	0.21	5.28	0.49	0.62	0.84
	Ambystoma	32	44	0.09	0.21	4.52	0.52	0.54	0.82
	Salamandra	32	42	0.08	0.17	4.67	0.49	0.63	0.82
	Celtedens	39	55	0.07	0.22	5.04	0.50	0.53	0.87
Pelvic	*Eryops*	37	51	0.08	0.14	4.93	0.54	0.57	0.84
	Balanerpeton	38	54	0.08	0.21	4.76	0.51	0.46	0.85
	Tulerpeton	46	59	0.06	0.11	5.81	0.51	0.63	0.85
	Ichthyostega	45	56	0.06	0.12	5.71	0.53	0.67	0.88
	Acanthostega	40	43	0.06	0.07	5.25	0.44	0.29	0.85
	Panderichthys	6	8	0.53	0.53	1.60	0.39	-0.20	0.44
	Eusthenopteron	9	8	0.22	0.00	2.56	0.55	-0.38	0.64
	Sterropterygion	9	8	0.22	0.00	2.56	0.55	-0.38	0.64
	Neoceratodus	63	84	0.04	0.38	5.47	0.97	-0.71	0.80
	Latimeria	22	33	0.14	0.29	2.81	0.55	0.16	0.76
	Polypterus	8	7	0.25	0.00	2.11	0.79	-0.59	0.63

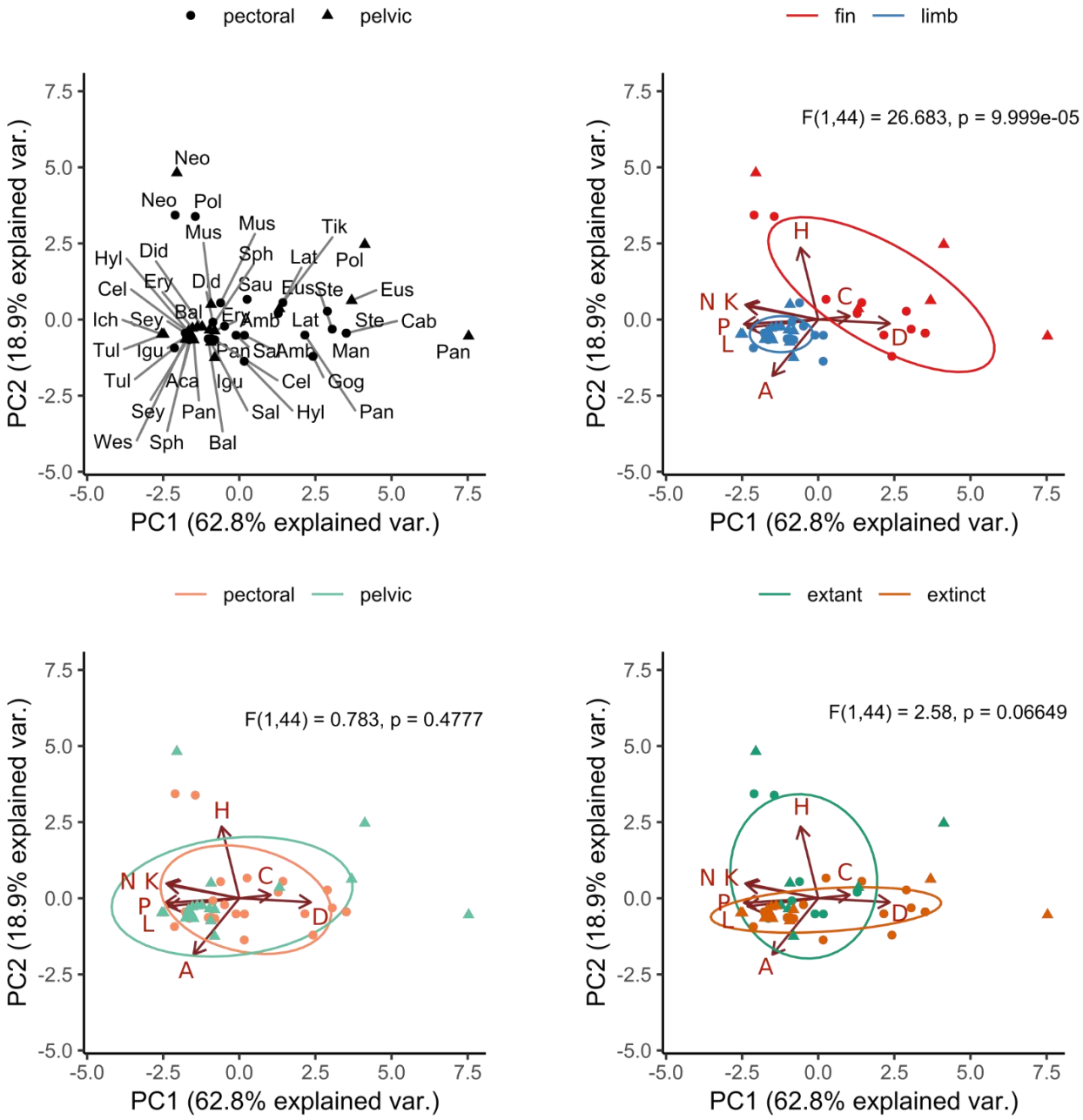

Fig. S12. Biplots of the first two PCA components of topological variables for pectoral (circles) and pelvic (triangles) appendages combined. Details in Fig. 2.

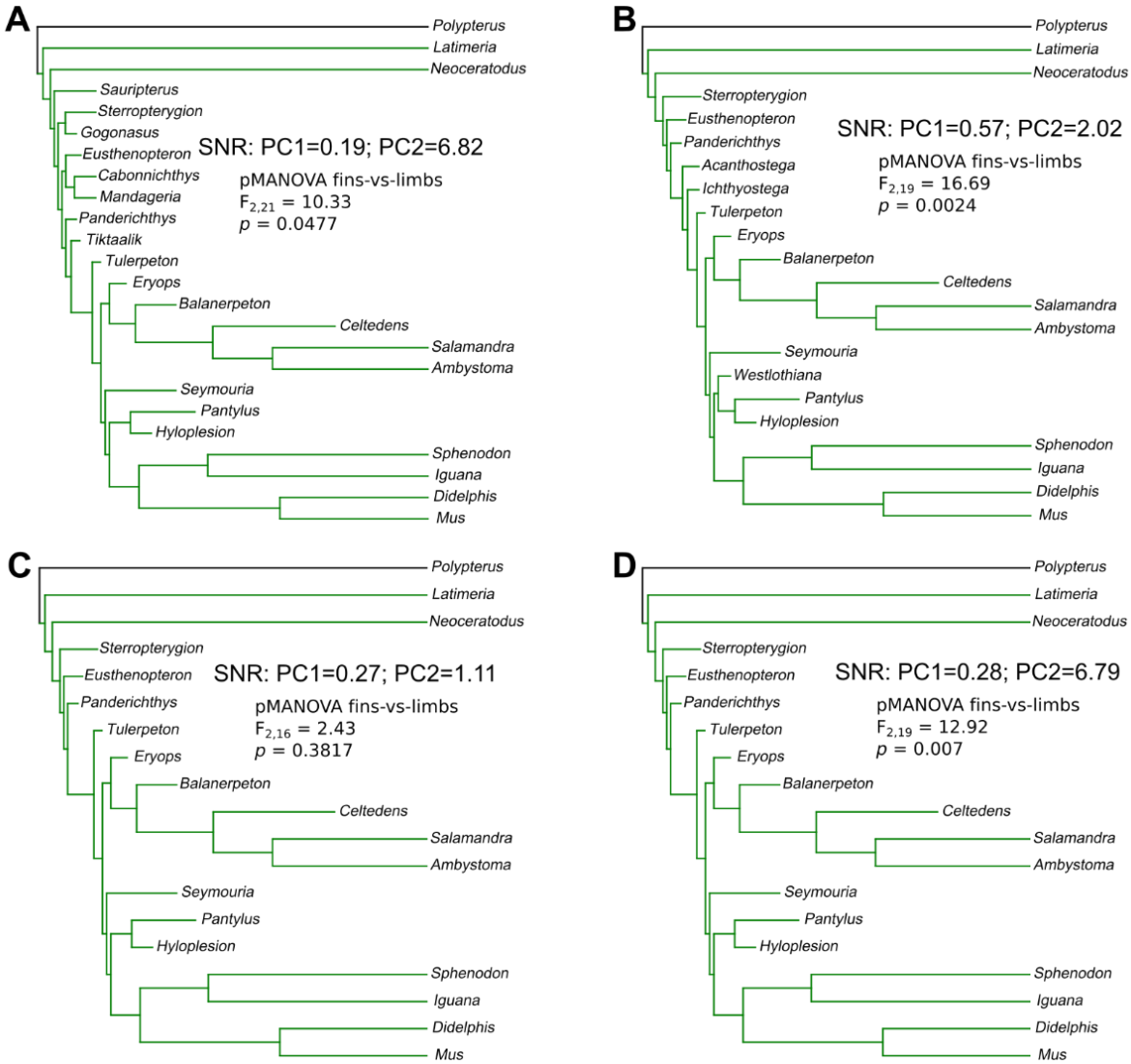

Fig. S13. Estimated evolutionary shifts using SURFACE. (**A**) Pectoral complete sample. (**B**) Pelvic complete sample. (**C**) Pectoral subsample. (**D**) Pelvic subsample. Details in Fig. 3.

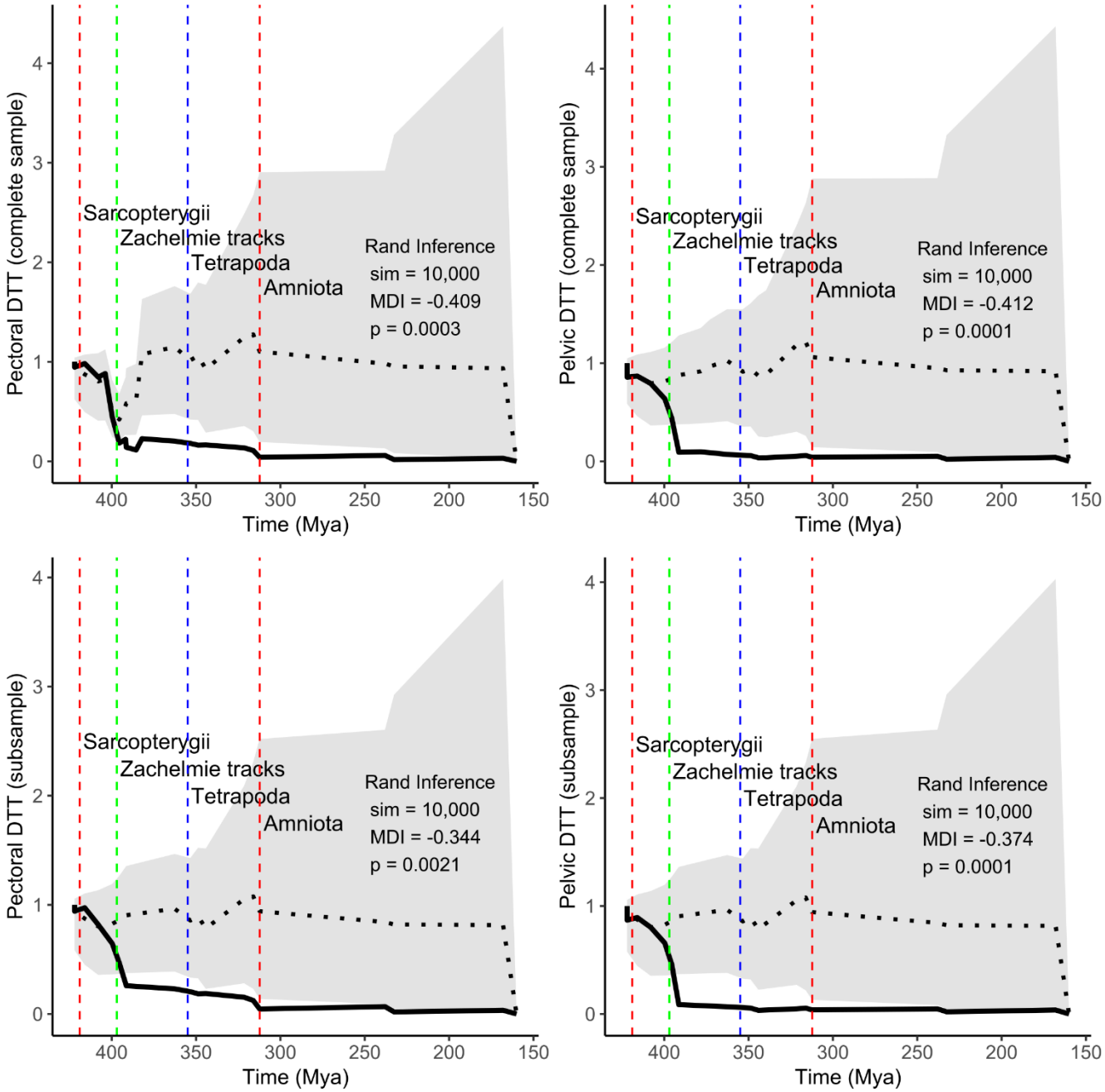

Fig. S14. Topological DTT for pectoral and pelvic appendages.

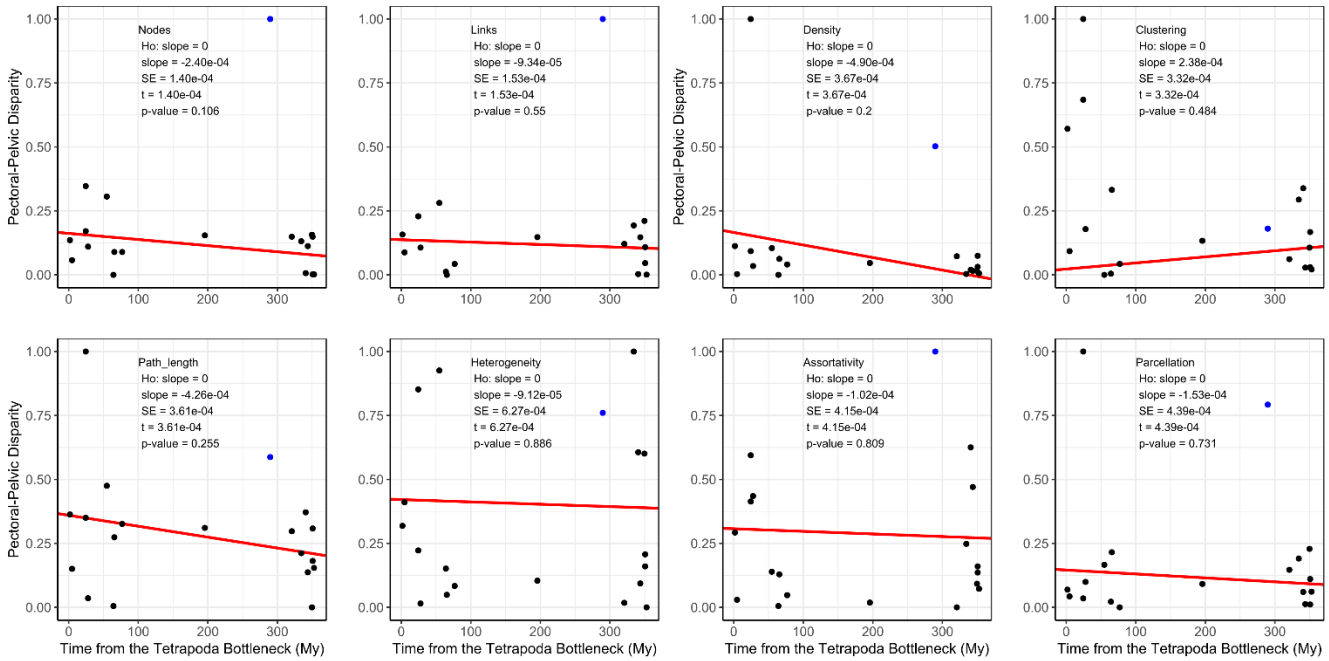

Fig. S15. Testing the pectoral-pelvic similarity bottleneck hypothesis for Tetrapoda. Phylogenetic Spearman's correlations were all non-significant (N, p = 0.86; K, p = 0.84; D, p = 0.62; C, p = 0.53; L, p = 0.96; H, p = 0.8; A, p = 0.38; and P, p = 0.54). Details in Fig. 5.